

## Synthesis of Superhydrophobic Carbon Surface during Combustion Propane

Z.A. Mansurov<sup>1\*</sup>, M. Nazhipkyzy<sup>1</sup>, B.T. Lesbayev<sup>1</sup>, N.G. Prikhodko<sup>1</sup>, M. Auyelkhankyzy<sup>1</sup>, I.K. Puri<sup>2</sup>

<sup>1</sup>Al-Farabi Kazakh National University, the Institute of Combustion Problems,  
050012, Bogenbay batyr street, 172, Almaty, Kazakhstan

<sup>2</sup>Department of Engineering Science and Mechanics, Virginia Tech, Blacksburg, Virginia 24061, USA

### Abstract

We synthesize and deposit carbon nanostructures through flame synthesis on silicon and nickel wafers at different nonpremixed flame locations to produce hydrophobic surfaces. The hydrophobicity is characterized through the contact angle for water droplets placed on the surface. The surface morphology of the nanoparticles is obtained from SEM images. The morphology and hydrophobicity of the nanostructured surfaces depends upon the deposition, which differs at various flame locations. We determine the optimum flame location for the synthesis and deposition of surface carbon nanostructures that lead to maximum hydrophobicity

### Introduction

Materials that are directly produced through combustion processes include carbon black, HCl, and TiO<sub>2</sub> [1]. Here, the flame provides precursors for the final product, e.g., hydrocarbons to produce solid carbon nanomaterials. The heat released during combustion can be adjusted by adding diluents and additives, and is thus a process control parameter. Low surface-energy materials like amorphous carbon (a-C) films can be produced in this manner [2-4]. These modify surfaces by altering their wettability [2-5] and contain carbon nanobeads that are morphologically similar to those catalyzed through hydrocarbon dissociation [2, 6].

Here, we describe method for the rapid deposition of a superhydrophobic soot film on nickel and silicon wafers by using a propane-oxygen nonpremixed flame. The burner configuration is identical to one used previously [2]. Water droplets placed on the surface of the carbon deposit have a large contact angle  $\theta$  in the 135-175° range.  $\theta$  is measured between the solid surface and the tangent at the point of contact between the liquid (water) and solid (combustion-generated carbon film) phases. Such a film is of practical interest as an anti-corrosion material that

mimics macromolecular coatings like Teflon, for instance, that typically has a wetting angle of 105-110°.

In course of the present work, we have developed an inedited technique for the carbon deposition on metals and semiconductors, based on the electric field application between the flame and substrate. We give here the preliminary results obtained with Si and Ni wafers.

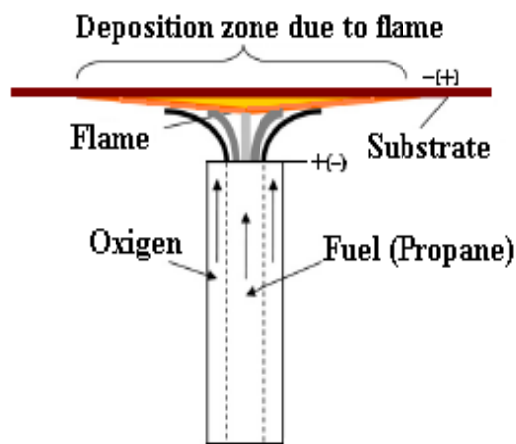
### Experimental method

A silicon (Si) disk is placed 2 cm above the burner, as shown in Fig. 1, and exposed to a flame for 4, 6 and 10 minutes. A nonpremixed flame is established using propane and oxygen flow rates between 50-150 cm<sup>3</sup>/min and 260-310 cm<sup>3</sup>/min, respectively, as described in Table 1 [7]. This results in the deposition of a carbon film, as shown in Fig. 2. The gas phase flame temperature just adjacent to the Si disk is measured to be 900°C with a chromel-alumel thermocouple of 0.2 mm diameter. The deposition occurs in three zones that are shown in Fig. 2, i.e., (1) a central gray area that is (2) surrounded by a brown zone, which (3) in turn is enclosed within a black sooty outer zone. (Figure 2 does not show these zones in the form of concentric circles due to minor flickering movements of the flame.)

\*corresponding author. Email: zmansurov@kaznu.kz



a



b

Fig. 1. Image and schematic representation of the burning experimental setup.

**Table 1**  
Experimental conditions for the synthesis of carbon deposits

Substrate	Propane flowrate (cm <sup>3</sup> /min)	Oxygen flowrate (cm <sup>3</sup> /min)	Substrate height above burner, (cm)	Exposure time, (min)
Si	51	260	2	4
	51	260	2	6
	51	260	2	10
	51	260	2	4
	51	260	2	6
	51	260	2	10
	70	285	3	6
	70	285	3	10
	150	310	2	10
	150	310	3	10
Ni	150	310	2	10

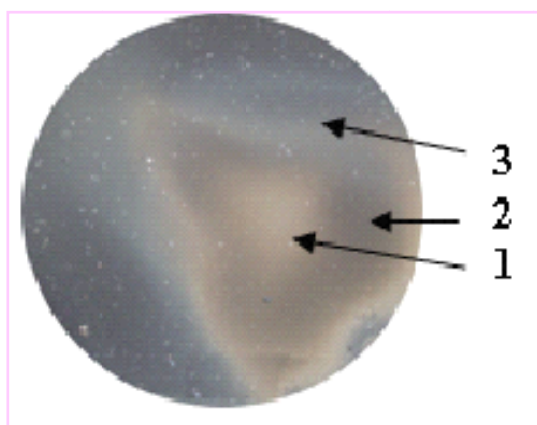


Fig. 2. A Si disc with carbon nanobead coating after 4 min exposure to the flame showing three deposition zones (1, 2 and 3).

Figure 3 represents images of liquid droplets placed on the central superhydrophobic region of the surface (Zone 1 in Fig. 2) and on a more hydrophilic bare Si wafer surface. A water droplet

placed on the hydrophobic surface is able to roll freely upon it. Regardless of the deposition time,  $\theta$  lies in the 152.4-157.1° range for such a surface and the coating is very stable. In the opposite the contact angle for the wettable bare Si wafer is equal to  $\theta = 50^\circ$ .

The deposited carbonaceous material has been examined using Raman spectroscopy. The Raman spectra recorded for different zones (identified in Fig. 2) are presented in Fig. 4. They all indicate the presence of various forms of carbon. Raman peak near 1350 cm<sup>-1</sup> (marked as D is due to amorphous-C, while the peak at 1590 cm<sup>-1</sup> (marked as G) is due to graphite. The most original aspect of the present study is the evidence of a new peak recorded at 1470 cm<sup>-1</sup> only for the two zones, 1 and 2. This peak has been attributed to the fullerene from of carbon. Figure 5 shows the scanning electron micrographs of two samples at the hydrophobic deposit (Zone 1). Both samples consist of similarly agglomerated nanobeads that are produced as a

result of gas phase fuel pyrolysis in the oxygen-deficient flame core. Heavier hydrocarbons in this central region of the flame are transported into the

stagnation layer adjacent to the relatively colder substrate where they condense and form the nanostructures.

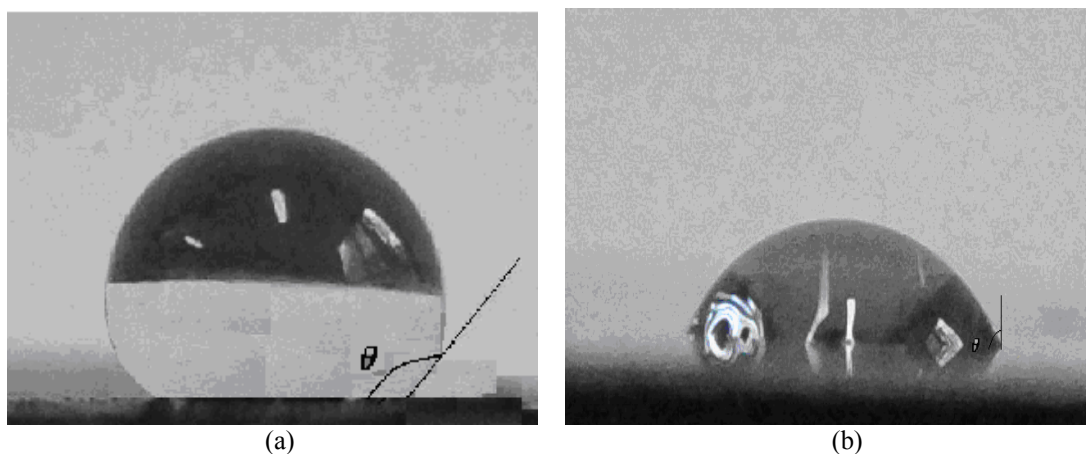


Fig. 3. (a) A drop of liquid placed on the central superhydrophobic region (zone 1) of the surface shown in Fig. 2, and (b) a more hydrophilic bare Si wafer surface.

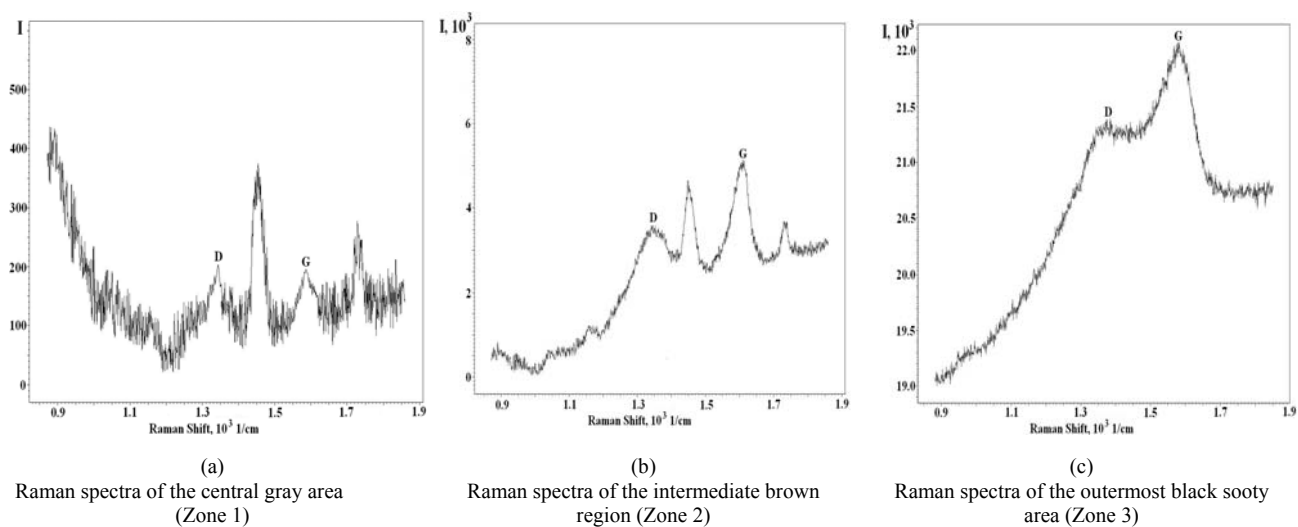


Fig. 4. Raman spectra of soot deposited on Si substrate. The ratio between the intensities of the G and the D peaks provides information about the lateral dimensions of the flakes.

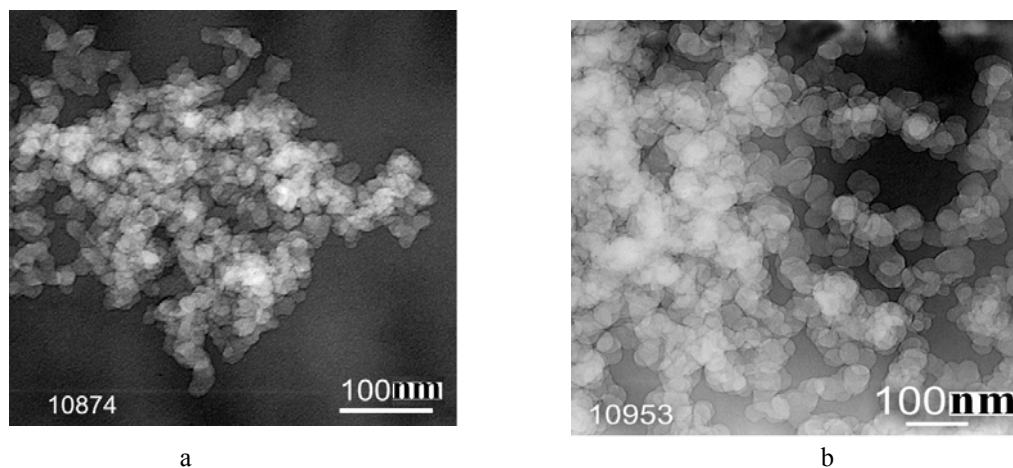


Fig. 5. Scanning electron micrographs of the chains formed with (a) and without (b) the application of a 1 kV electric field during the carbon deposit in Zone 1 (Fig.2).

We next investigated the influence of an electric field of 1 kV strength that is applied between the substrate and the burner rim for 10 min. Substrates thus exposed are compared with others exposed to the same flame in the absence of such a field. For all these cases, the flame is established with propane and oxygen flowrates of 51 and 260  $\text{cm}^3/\text{min}$ , respectively. For this flame, Zones 1 and 2 contain carbon nanobead chains that are 15-30 nm long in the absence of an electric field. This chain length increases to 40-50 nm when the field is applied. In all cases, the outermost Zone 3 contains coagulated soot aggregates that have characteristic sizes of 30-50 nm.

When an electric field (of 1 kV) is applied to either the Si or Ni substrate, the flame changes visually and becomes brighter. It contains a periodic spark that jumps between the burner rim and the substrate. Then the soot formation in the flame is enhanced. The increase in flame soot decreases the electric resistance of the flame which results in the increase of the electric current through the flame. Large quantities of soot are deposited on the substrate in the form of dendrites, increasing the thickness of the hydrophobic deposit for this case. While a normal flame, i.e., one established in the absence of an electric field, spreads over the surface of the substrate, in the presence of an electric field, it propagates as a narrower cylinder of 1.5 cm diameter, even as it touches the substrate. When the substrate has a negative polarity, the flame adheres to it. A corresponding positive polarity produces a small gap between the flame front and substrate, in which case the Zone 1 superhydrophobic deposit exhibits a larger wetting angle of 160-165°.

We have also investigated the interactions of three surfactants with the resulting hydrophobic soot surface on a silicon substrate, namely (1) the anionic sodium dodecyl sulfate ( $\text{C}_{12}\text{H}_{25}\text{OSO}_3\text{Na}$ ), (2) the cationic tsetilperidiniya bromide ( $\text{C}_{16}\text{H}_{33}\text{C}_5\text{H}_5\text{N Br}$ ), and (3) the nonionic oxyethylenated alkylphenol ( $\text{C}_{16}\text{H}_{33}\text{C}_6\text{H}_4\text{O}(\text{CH}_2\text{CH}_2\text{O})_{10}\text{H}$ ).

In a second step, we investigate the influence of surfactants on the hydrophobicity of the deposit in Zone 1. The modifying effect of the anionic sodium dodecyl sulfate ( $\text{S}_{12}\text{H}_{25}\text{OSO}_3\text{Na}$ ), cationic tsetilperidiniya bromide ( $\text{C}_{16}\text{H}_{33}\text{C}_5\text{H}_5\text{N Br}$ ) and nonionic alkylphenol oxyethylenated ( $\text{C}_{16}\text{H}_{33}\text{C}_6\text{H}_4\text{O}(\text{CH}_2\text{CH}_2\text{O})_{10}\text{H}$ ) surfactants was considered. The wetting angles obtained as the surfactant concentration is varied are presented in Fig. 6. This

figure shows that the required hydrophobicity or hydrophilicity of the substrates can be modified by varying the surfactant concentration in water.

We also carried out the study of the conditions of surfactants interaction with obtained hydrophobic soot surface on substrates. The modifying effect of anionic - sodium dodecyl sulfate ( $\text{S}_{12}\text{H}_{25}\text{OSO}_3\text{Na}$ ), cationic - tsetilperidiniya bromide ( $\text{C}_{16}\text{H}_{33}\text{C}_5\text{H}_5\text{N Br}$ ) and a nonionic surfactant - alkylphenol Oxyethylenated ( $\text{C}_{16}\text{H}_{33}\text{C}_6\text{H}_4\text{O}(\text{CH}_2\text{CH}_2\text{O})_{10}\text{H}$ ) analysed. On the basis of experimental data, the diagram dependence of wetting angle versus the logarithm of surfactant concentration was made by the plot of the contact angle versus of the logarithm of surfactant concentration (Fig. 6).

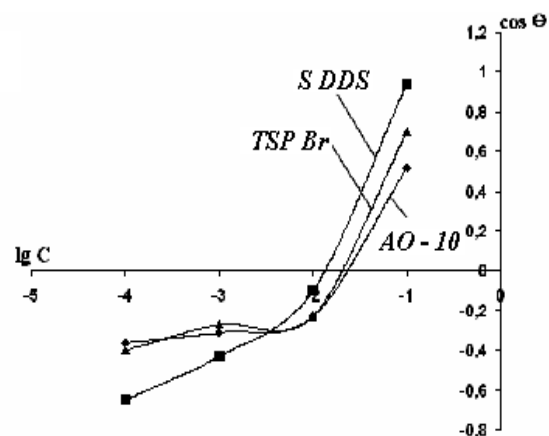


Fig. 6. Variation of the contact angle versus the logarithm of concentration

## Conclusions

The present study has evidenced the formation of fullerenes and carbon nanotubes as well as soot with the superhydrophobic surface, using both nickel and silicon substrates in benzene-oxygen or propane-oxygen diffusion flames. New results regarding the synthesis of superhydrophobic surface with a contact angle of 135-175° have been found with great practical interest as anti-corrosion additives to various materials.

We have also shown that the use of surface-active substances can specifically regulate the hydrophobic properties of the carbon black surface to the desired degree of hydrophilicity. The modifying rate of surface active substances is determined by the degree of hydration of polar groups.

**References**

1. Z.A. Mansurov. Some applications of nanocarbon materials for novel devices / R. Gross et. al (eds.), *Nanoscale Devices - Fundamentals and Applications*, 355-368. 2006 Springer.
2. S. Sen, I.K. Puri Flame synthesis of carbon nanofibers and nanofiber composites containing encapsulated metal particles. *Nanotechnology* 2004; 15 (3): 264 - 8.
3. S. Naha., S. Sen, I.K. Puri. Flame synthesis of superhydrophobic amorphous carbon surfaces, *Carbon V. 45, Issue 8, (2007)*, P. 1702-1706.
4. S. Mazumder., S. Ghosh., I. Puri. Nonpremixed flame synthesis of hydrophobic carbon nanostructured surfaces, 33 th. Symp. (Intern.) on Combustion. Pittsburgh: The Combustion Inst., (2010).
5. J. Robertson Diamond-like amorphous carbon. *Mater Sci Eng R* 2002; 37 (4 - 6): 129 - 281.
6. A. Levesque, V.T. Binh, V. Semet, D. Guillot, R.Y. Fillit, M.D. Brookes, et al. Mono disperse carbon nanopearls in a foam-like arrangement: a new carbon nano-compound for cold cathodes. *Thin Solid Films* 2004; 464-465: 308 - 14.
7. Z.A. Mansurov, M. Nazhipkyzy, B.T. Lesbaev, I.K. Puri. Synthesis of superhydrophobic carbon surface during combustion propane. *Oil and Gas, (2010)*; 5; p. 27-33 (In Russian).

*Received 24 August 2011*